

Joint PP-PS inversion at Pikes Peak oilfield, Saskatchewan

Hongbo Zhang*, Gary F. Margrave, and R. James Brown
Dept. of GLGP, University of Calgary,
2500 university drive NW, Calgary, AB, T2N 1N4
hzhang@geo.ucalgary.ca

ABSTRACT

The method of simultaneous PP-PS inversion has recently been developed and tested on the 3-D Blackfoot seismic data set. This paper shows the application of this method on 3C-2D seismic data from Pikes Peak oilfield. The inversion was accomplished with a newly installed inversion module in ProMAX. After careful prestack processing, five limited-offset stacked sections for each of the vertical and radial components were created, migrated and correlated. The inversion module assumes that the data have been trace- equalized and, to restore the average AVO behaviour, it requires the input of scalar RMS amplitude estimates for each offset. These were obtained by creating elastic synthetic seismograms for P-P and P-S from well control and calculating the RMS amplitudes for each offset. Then the ten datasets, together with the RMS amplitude values and a background velocity model, were input into the joint PP-PS AVO inversion module in ProMAX. The weighted stacking requires estimation of the P-P and P-S incidence angles at each depth level and this is done by raytracing through the background velocity model. Four attributes were determined: fractional P-wave impedance $\Delta I/I$, fractional S-wave impedance $\Delta J/J$, $\Delta(\lambda\rho)/\lambda\rho$ and $\Delta(\lambda/\mu)/(\lambda/\mu)$. Good correlation of these parameters from seismic inversion and those calculated from well logs shows that simultaneous PP-PS AVO inversion can be used to indicate anomalous lithology and pore-fluid changes in the subsurface. Therefore it should be helpful in detecting hydrocarbons using 2-D multicomponent seismic data.

Introduction

Geology

Pikes Peak oilfield is a heavy-oil field located 40 km east of Lloydminster, Saskatchewan (Figure 1). It has been operated by Husky Energy Ltd. since 1981 and over 35 million barrels have been produced. Steam-drive technology has been used to enhance recovery. The principle of steam drive is to reduce the effective viscosity of the oil and increase the mobility in the reservoir by injecting high-temperature and -pressure steam.

Sediments of the Lower Cretaceous Mannville Gp overlie the pre-Cretaceous unconformity developed on gently southwesterly-dipping Paleozoic strata. Post-Mannville tilting to the southwest has enhanced the structural dip on the subcropping Paleozoic strata in the Lloydminster area (Orr et al., 1977). Dissolution of deep Devonian salt units around the flanks of the field set up the combination structural and stratigraphic trap. The two major producing reservoirs

in the Pikes Peak field are the General Petroleum Fm and the Waseca Fm (Van Hulten, 1984). This study discusses only the Waseca oil sands that are located in the Mannville Gp and about 480 m below the surface of the Earth.

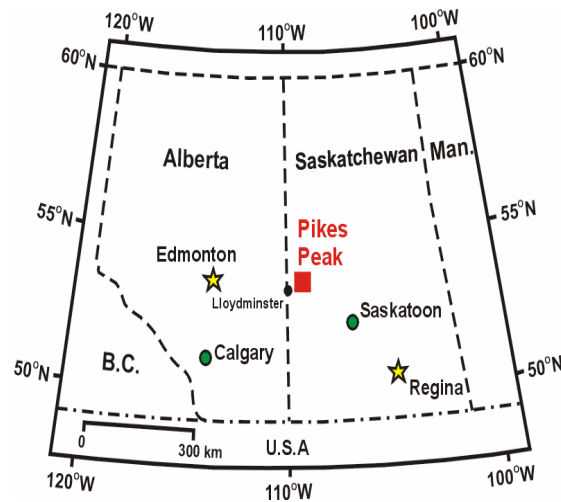


FIG. 1: Location map of the Pikes Peak oil field (edited from Hoffe et al., 2000).

The coal and sideritic shale in the McLaren and the shale at the top of the Waseca Fm form the perfect seal for the hydrocarbon in shale/sand interbed and homogeneous sand units (Van Hulten, 1984) in the middle and lower Waseca. The up-fining depositional sequences in Figure 2 demonstrate typical channel facies. The main producing zone within the Waseca Fm is the homogeneous sand unit. It ranges between 5 and 30 m of net pay within the field. The coal at the top of the Sparky Fm forms a horizon that is resistive to channel erosion. The positions of the four wells are shown in Figure 3.

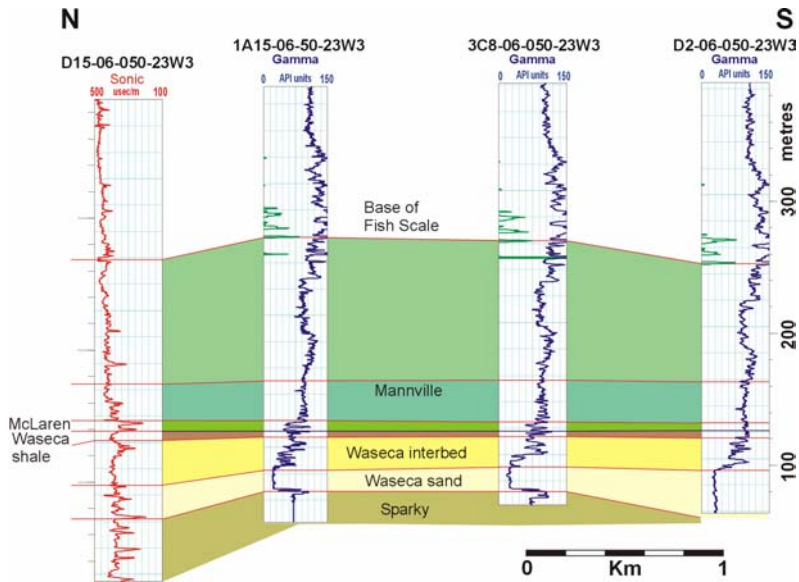


FIG. 2: Well-log cross-section illustrating the Lower Cretaceous stratigraphy (flattened at the top of the Waseca Fm). There is a channel sequence previously interpreted within the Waseca Fm (Van Hulten, 1984) and refined by the authors.

Seismic and Well-Log Data

The seismic data used in this inversion project were acquired on the eastern side of the field (Figure 3) in March 2000 by the University of Calgary AOSTRA (Alberta Oil Sands Technology Research Authority) group and Husky Energy Ltd. and processed at Matrix Geoservices Ltd. For the vertical- and radial-component data used in this project, the processing from offset arrangement to inversion was performed by the authors and the processing before this study was carried out by Matrix Geoservices Ltd.

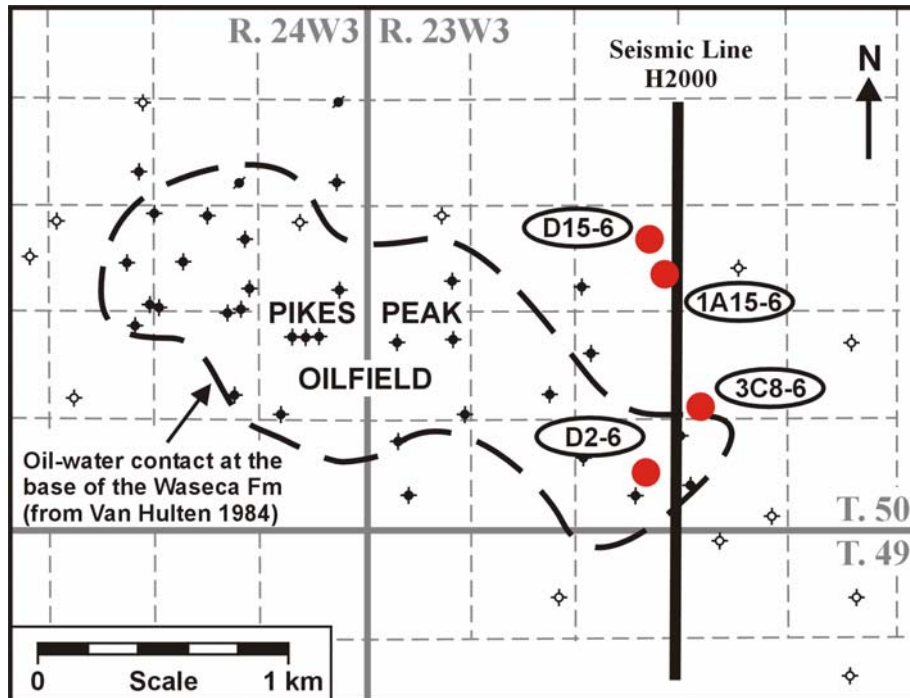


Fig. 3: Location map of the seismic line and the four wells used in this project.

While the seismic data were being acquired, pump jacks for hydrocarbon production were running constantly. The noise from pump jacks does not show up in the vertical-component data because of their high frequencies (2-150 Hz). But the noise does show up in the radial-component data due to their much lower frequencies (2-60 Hz). This is why an $f-k$ filter was applied to the radial component. Careful attention was also paid to the large receiver statics present in the radial-component dataset. To solve this problem, the common-receiver stack was created so that the reflectors with small lateral changes in time were corrected. After that, residual source and receiver statics were calculated and eliminated.

The wells 1A15-6, D15-6, 3C8-6 and D2-6 were used to create synthetic P-P seismograms to tie to the P-wave seismic data due to the fact that these wells had original sonic and density logs over the Waseca interval. Well 1A15-6 was also used to tie to the converted-wave (P-S) seismic data because it had a dipole sonic log. For these data, constant-phase rotations of -45° and 90° were applied to the vertical- and radial-component data so as to give an optimal match to the synthetics.

Methodology

The technique of joint PP-PS weighted stacking is used in the course of inversion. Stewart (1990) developed this method and Larsen et al. (1998), Larsen (1999) and Margrave et al. (2001) provided its first practical applications. The method requires migrated common-image-point gathers for both P-P and P-

S reflections. These are then summed into a weighted stack, where the weights are derived from a smoothed background velocity model, to estimate fractional P and S impedance. The resulting sets of stacked sections are estimates of changes in $\Delta I/I$ and $\Delta J/J$. From these weighted stacks, such useful elastic parameters $\Delta(\lambda\rho)/\lambda\rho$ and $\Delta(\lambda/\mu)/(\lambda/\mu)$ can be derived. For the mathematical basis of this method, see Larsen (1999).

The physical basis for the method is embodied in the first-order Zoeppritz-equation approximations for plane-wave reflection and transmission coefficients. The approximations are made under the assumptions that two solid half-spaces are welded at an elastic interface, that there are only small relative changes in elastic parameters, and that the average P- and S-wave angles of incidence and transmission across the interface do not approach a critical angle or 90° (Aki and Richards, 1980). The plane-wave assumption is one that can cause inaccurate estimation of near-offset data.

The implementation of this method can be generalized as follows. First, the 3C-2D seismic data were acquired and processed to obtain high-quality, true-relative-amplitude prestack seismic data volumes. Rather than performing a full prestack migration, we NMO corrected and stacked these into limited-offset volumes that could be post-stack migrated. Five of such limited-offset, migrated sections were created for both P-P and P-S reflections. Because true-amplitude recovery in regular processing is not perfect, synthetic seismograms for each reflection type were used to restore the average behaviour of reflectivity with offset. These were constructed from well logs by raytracing for the traveltimes and using the Zoeppritz equations for the reflection calculations. They were then band-limited to the recovered signal band of the data. Then the expected RMS amplitude for each offset range was calculated from the P-P and P-S synthetic seismograms. Each limited-offset migrated data volume was then rescaled by a constant factor to have the same RMS amplitude as the corresponding synthetic seismogram. Second, offset ranges were chosen to create limited-offset stacked sections so that the volume of data needed for AVO analysis would be smaller and both the speed of calculation and the signal-to-noise ratio would be increased. Since migration was also applied to the stacked sections, the quality of imaging was greatly improved. Third, P-P and P-S reflection events were correlated in depth by comparing them to the synthetic seismograms. Finally, each offset data volume was weighted and they were summed together to estimate fractional P or S impedance. For example, the fractional P-wave impedance is given by:

$$\frac{\Delta I}{I} = \sum_{offset} data \times weights . \quad (1)$$

where the sum includes both P-P and P-S data, the weights are functions of the average incidence and reflection angles for smooth P-wave and S-wave velocity-

depth models and where raytracing is used to determine the incidence, reflection and transmission angles. The formulae for the weights are quite complex and are not reproduced here. They may be found in Larsen (1999).

The software that carries out the simultaneous PP-PS inversion is a module called joint P-P and P-S AVO inversion in ProMAX created by X. Li in 2000 and updated and documented by D. Henley in 2002. Software packages SYNTH and LOGEDIT (CREWES proprietary software) were used to create the synthetic seismograms, Well Editor, GeoGraphix, Model Builder and CorelDraw were also used in the course of this research and the composition of this paper.

Correlation of seismic inversion and well log computation

In this paper, in order to test whether the method of joint PP-PS AVO inversion is effective, especially the zone of interest shown in Figure 4, correlation of the results from seismic inversion and impedance estimates calculated from well logs was conducted. In order to decide how effective joint PP-PS AVO inversion is, the results from P-P stand-alone inversion are also

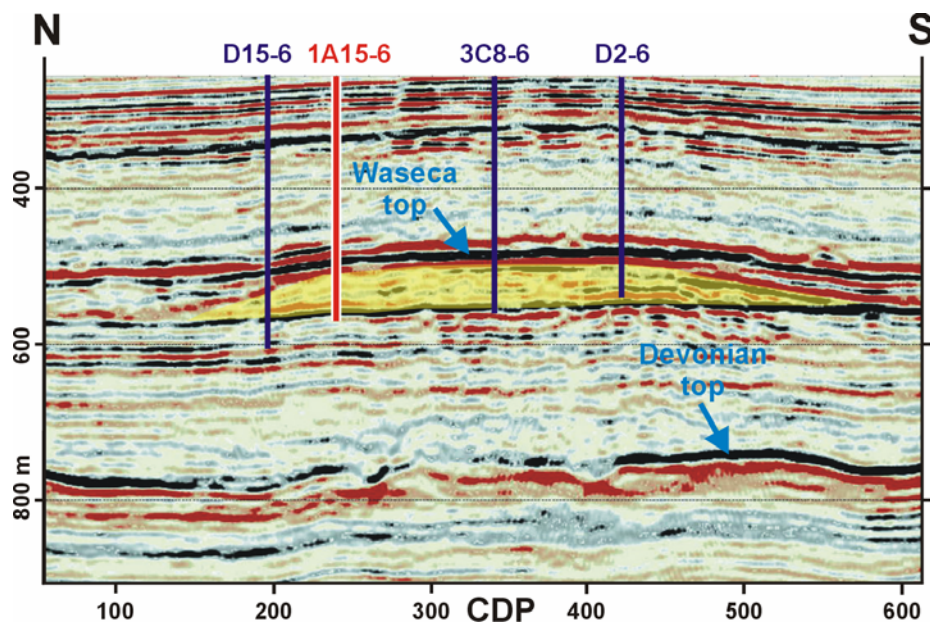


Fig. 4: The Waseca Fm reservoir (in yellow) and wells, including the dipole well 1A15-6 used in this paper.

correlated to the direct well-log computations respectively. P-P stand-alone inversion is to simply examine the case of a P-P reflection and extract lithology and pore-fluid parameters from P-P seismic data only. In this case, all weights and reflectivities except weights in P-P reflectivity are set to zero. However, the P-P weights for P-P only inversion are different from the P-P weights for joint PP-PS inversion.

Fractional impedance calculation from well logs

Since the frequencies of well-log data are much higher than those of seismic data, the well logs must be smoothed and downsampled (Figure 5) to make them directly comparable with the seismic data. First, the well-log sampling interval (dz_2) was increased by local averaging and decimation. The well logs were averaged over 4-m intervals for better $\Delta I/I$ and $\Delta J/J$ correlation with the results from seismic inversion. Second, the fractional impedances (P and S) are generated from these downsampled data according to equations (2) to (3) and (4) to (5) (Goodway et al. 1997), by taking ratios of the difference and average of consecutive pairs of samples:

$$\text{Fractional P-wave impedance: } \frac{\Delta I}{I} = \frac{2(I_2 - I_1)}{I_2 + I_1} \quad (2)$$

$$\text{Fractional S-wave impedance: } \frac{\Delta J}{J} = \frac{2(J_2 - J_1)}{J_2 + J_1} \quad (3)$$

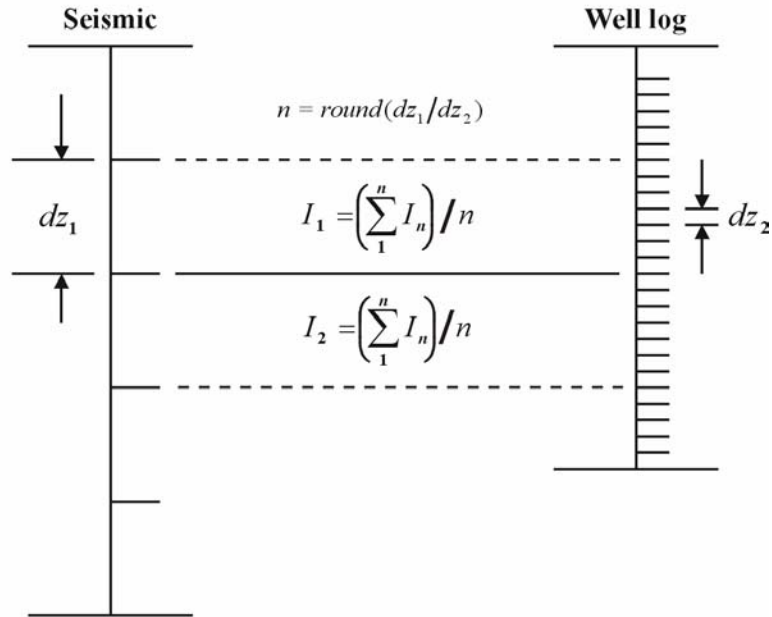


FIG. 5: An example of how the well log is downsampled to calculate fractional P-wave impedance.

$$\text{Fractional } \lambda\rho: \quad \frac{\Delta(\lambda\rho)}{\lambda\rho} = \frac{2}{\alpha^2 - 2\beta^2} \left(\alpha^2 \frac{\Delta I}{I} - 2\beta^2 \frac{\Delta J}{J} \right) \quad (4)$$

$$\text{Fractional } \lambda/\mu: \quad \frac{\Delta(\lambda/\mu)}{\lambda/\mu} = \frac{2\alpha^2}{\alpha^2 - 2\beta^2} \left(\frac{\Delta I}{I} - \frac{\Delta J}{J} \right) \quad (5)$$

where α and β are the average P-wave and S-wave velocities across the interface, $I = \rho\alpha$, $J = \rho\beta$.

Results of correlation

The well-log computation was tied PP-PS simultaneous inversion and P-wave only inversion respectively (Figures 6-7). Generally, the correlation

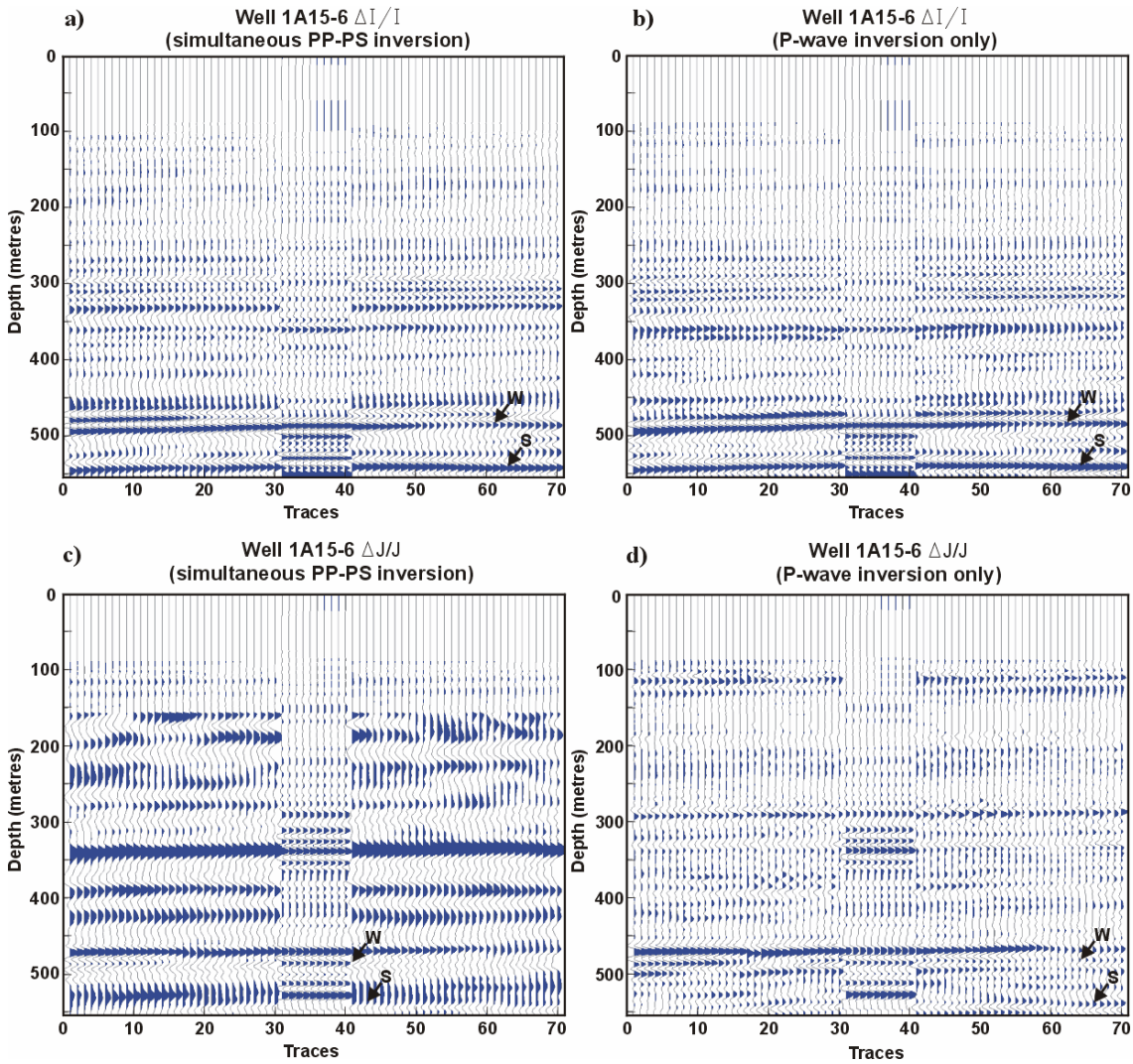


Fig. 6: Well 1A15-6 correlation of $\Delta I/I$ and $\Delta J/J$ from seismic inversion and well-log computation. **W**-Waseca top; **S**-Sparky top.

between simultaneous inversion and well-log computation for well 1A15-6 is quite good. In comparison, the results of P-wave only inversion are similar for P-wave impedance but quite different for S-wave impedance. It seems that the joint inversion S-wave estimates are more coherent but also lower resolution. We do not yet know the reason for this reduced bandwidth but speculate that it is a

consequence of the lower bandwidth of the P-S data. Despite this lower bandwidth, the S-wave impedance estimate from joint inversion ties the well control better than that from P-P only. Especially, the channel sequence within the zone of interest between Waseca top and Sparky top is better imaged by the joint inversion.

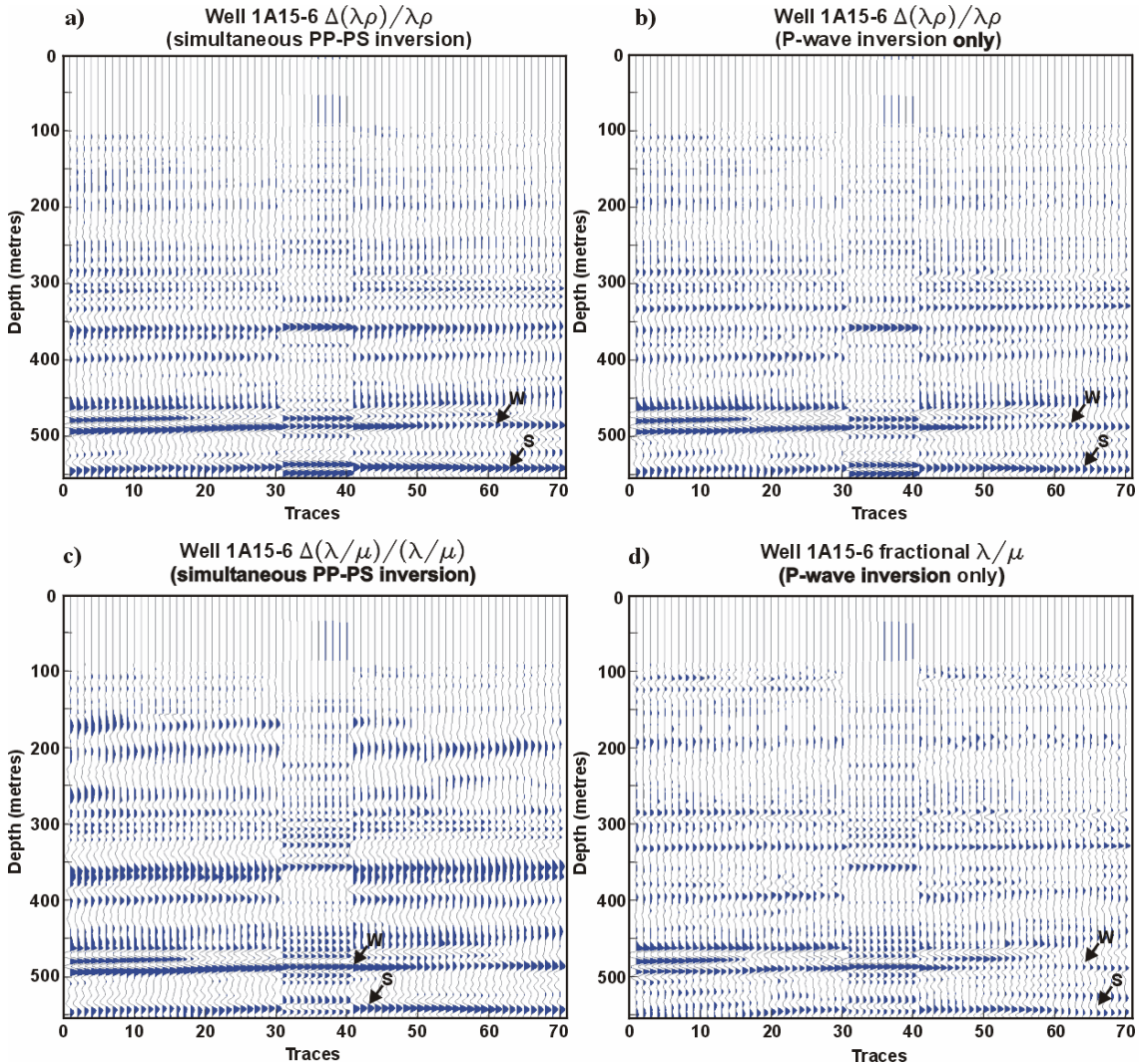


FIG. 7: Well 1A15-6 correlation of $\Delta(\lambda\rho)/\lambda\rho$ and $\Delta(\lambda/\mu)/(\lambda/\mu)$ from seismic inversion and well-log computation, **W**-Waseca top; **S**-Sparky top.

Meanwhile, among the four attributes obtained by inversion, $\Delta I/I$ and $\Delta(\lambda\rho)/\lambda\rho$ are of higher frequencies and better imaging quality because they are more highly dependent upon P-P reflectivity. On the contrary, $\Delta J/J$ and $\Delta(\lambda/\mu)/(\lambda/\mu)$ are of lower frequencies because they are more dependent on shear impedance contrasts. In places where there are hydrocarbons, $\Delta I/I$ and $\Delta(\lambda\rho)/\lambda\rho$ change relatively more than $\Delta J/J$ and $\Delta(\lambda/\mu)/(\lambda/\mu)$.

There are some misties between seismic inversion and well-log computation in either the shallow part or the part that is close to the datum. The latter may be due to phase differences between seismic and well-log computation and the steam-injection that was going on in other nearby wells. The former may be due to both lower fold for shallow seismic data and phase differences.

Conclusions

A joint P-P and P-S inversion was conducted on a 2-D multicomponent seismic line over the Pikes Peak field. The inversion required creation of migrated, limited-offset sections for both P-P and P-S data and generation of synthetic seismograms from well control. Approximate relative amplitude restoration of the seismic data was accomplished by equalizing its RMS amplitudes with those of the synthetic seismograms for each offset. Then fractional P and S impedances were estimated by forming weighted stacks of the migrated, limited-offset sections. The success of the inversion was judged by comparing the estimated fractional impedances with direct calculations from wells.

By virtue of good correlation between simultaneous inversion and well-log computation, we conclude that the method of joint PP-PS AVO inversion worked well in this case. This could prove helpful in indicating anomalous lithology and pore-fluid changes in the subsurface and, thereby, in oil and gas exploration, since information contained in both P-wave and S-wave seismic data is utilized in detecting these seismic anomalies.

Acknowledgements

The authors gratefully acknowledge the support of the CREWES sponsors, discussions with Dave Henley, Hanxing Lu and Ian Watson concerning the simultaneous inversion and the Pikes Peak oilfield, and help from Henry Bland and Kevin Hall on the computer system.

References

Aki, K., and Richards, P.G., 1980, Quantitative seismology: Theory and Methods: W.H. Freeman and Company, Vol. 1.

Goodway, B., Chen, T., and Downton, J., 1997, Improved AVO fluid detection and lithology discrimination using Lamé petrophysical parameters: " $\lambda\rho$ ", " $\mu\rho$ " and " $\lambda\mu$ fluid stack", from P and S inversions: CSEG Expanded Abstracts, 148-151.

Hoffe, B.H., Bertram, M.B., Bland, H.C., Gallant, E.V., Lines, L.R., and Mewhort, L.E., 2000, Acquisition and processing of the Pikes Peak 3C-2D seismic survey, CREWES Research Report, **12**, 511-522.

Larsen, J.A., Margrave, G.F., Lu, H., and Potter, C.C., 1998, Simultaneous P-P and P-S inversion by weighted stacking applied to the Blackfoot 3C-3D survey, CREWES Research Report, **10**, 50, 1-23.

Larsen, J.A., 1999, AVO inversion by simultaneous P-P and P-S inversion: M.Sc. Thesis, University of Calgary.

Margrave, G.F., Stewart, R.R., and Larsen, J.A., 2001, Joint PP and PS seismic inversion: The Leading Edge, **20**, 1048-1052.

Orr, R.D., and Johnston, J.R., Manko, E.M., 1977, Lower Cretaceous geology and heavy-oil potential of the Lloydminster area: Bulletin of Canadian Petroleum Geology, **25**, 1187-1221

Stewart, R.R., 1990, Joint P and P-SV inversion: CREWES Research Report, **2**, 112-115.

Van Hulten, F.F.N., 1984, Petroleum geology of Pikes Peak heavy oil field, Waseca Fm, Lower Cretaceous, Saskatchewan, Canadian Society of Petroleum Geologists, Memoir 9, 441-454.